Supplementary Information

Canting Angle Dependence of Single-Chain Magnet Behaviour in Chirality-Introduced Antiferromagnetic Chains of Acetate-Bridged Manganese(III) Salen-Type Complexes

Po-Jung Huang[†] and Hitoshi Miyasaka*[†,‡]

[†] Department of Chemistry, Graduate School of Science, Tohoku University, 6-3 Aramaki-Aza-Aoba, Aoba-ku, Sendai 980-8578, Japan

[‡] Institute for Materials Research, Tohoku University, 2-1-1 Katahira, Aoba-ku, Sendai 980-8577, Japan

* Corresponding author:
Hitoshi Miyasaka
Institute for Materials Research, Tohoku University, 2-1-1 Katahira, Aoba-ku, Sendai 980-8577, Japan
Tel: +81-22-215-2030
Fax: +81-22-215-2031
e-mail: miyasaka@imr.tohoku.ac.jp

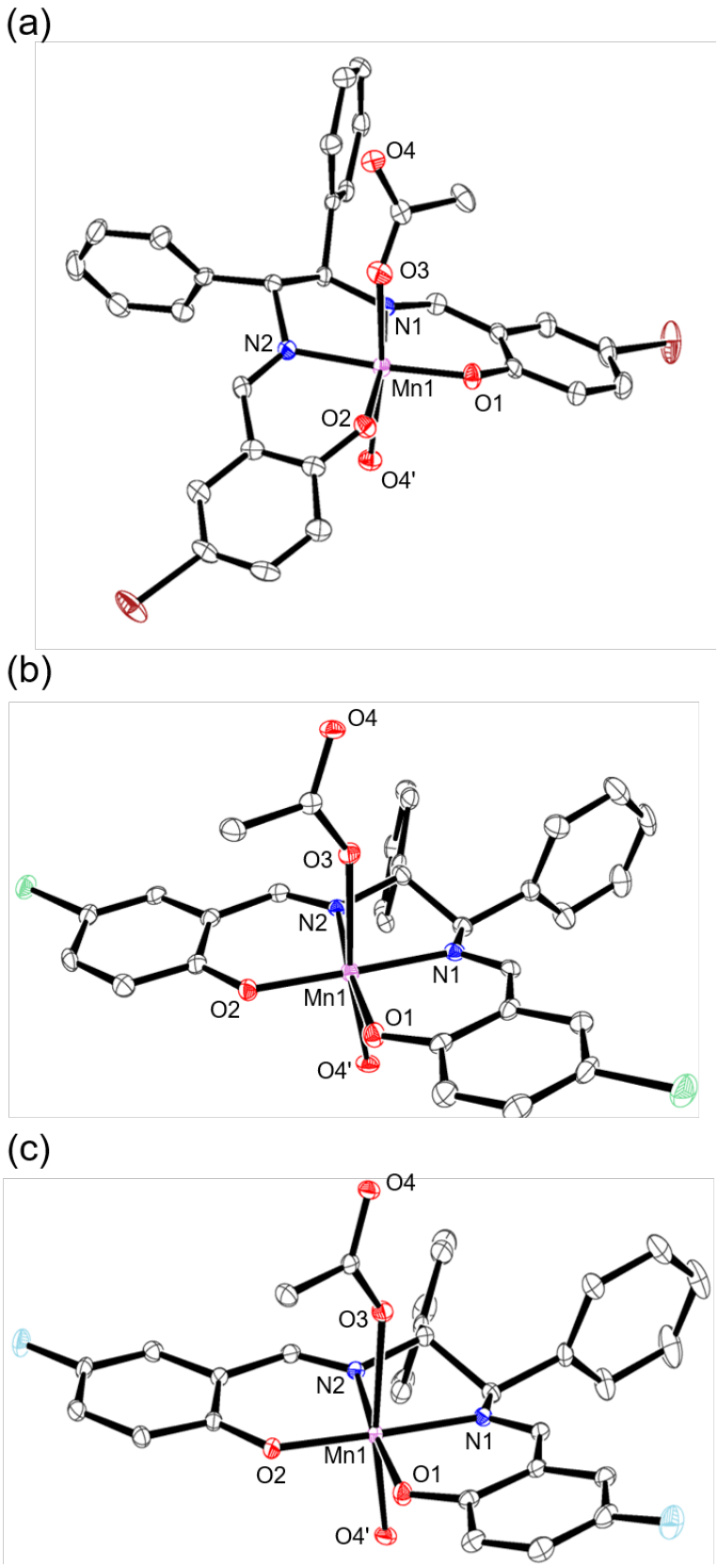

Figure S1. ORTEP drawings of core structure of ***RR*-1** (a), ***RR*-2** (b), and ***RR*-3** (c), where colour codes: Mn (purple), O (red), N (blue), C (grey), Br (brown), Cl (green), F (turquoise), and H atoms were omitted for clarity.

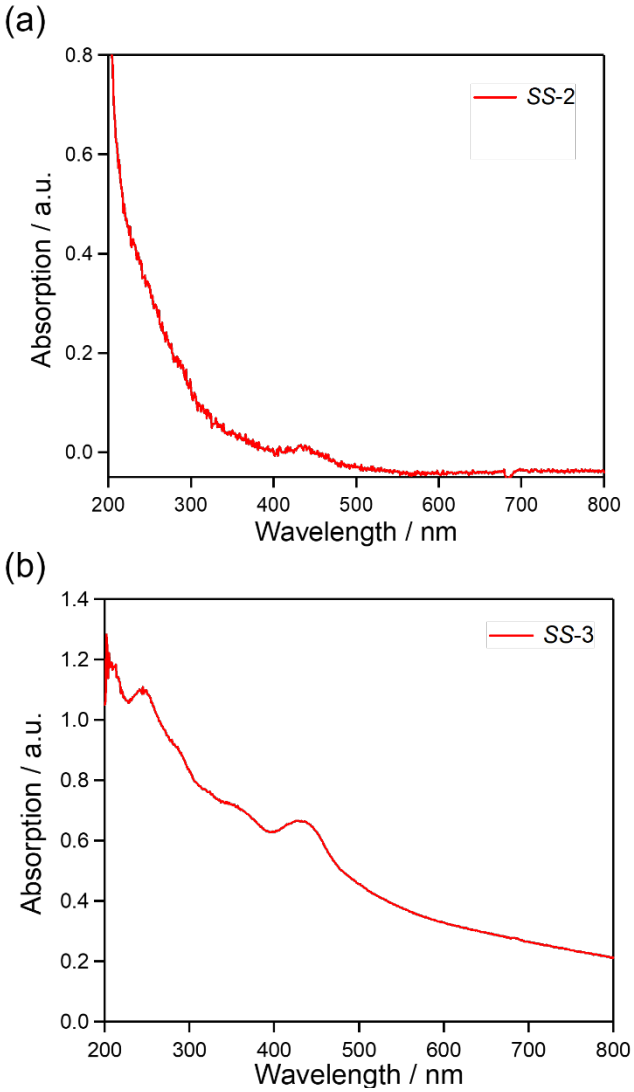

Figure S2. Absorption spectra of ***SS*-2** (a) and ***SS*-3** (b) collected in KBr pellet.

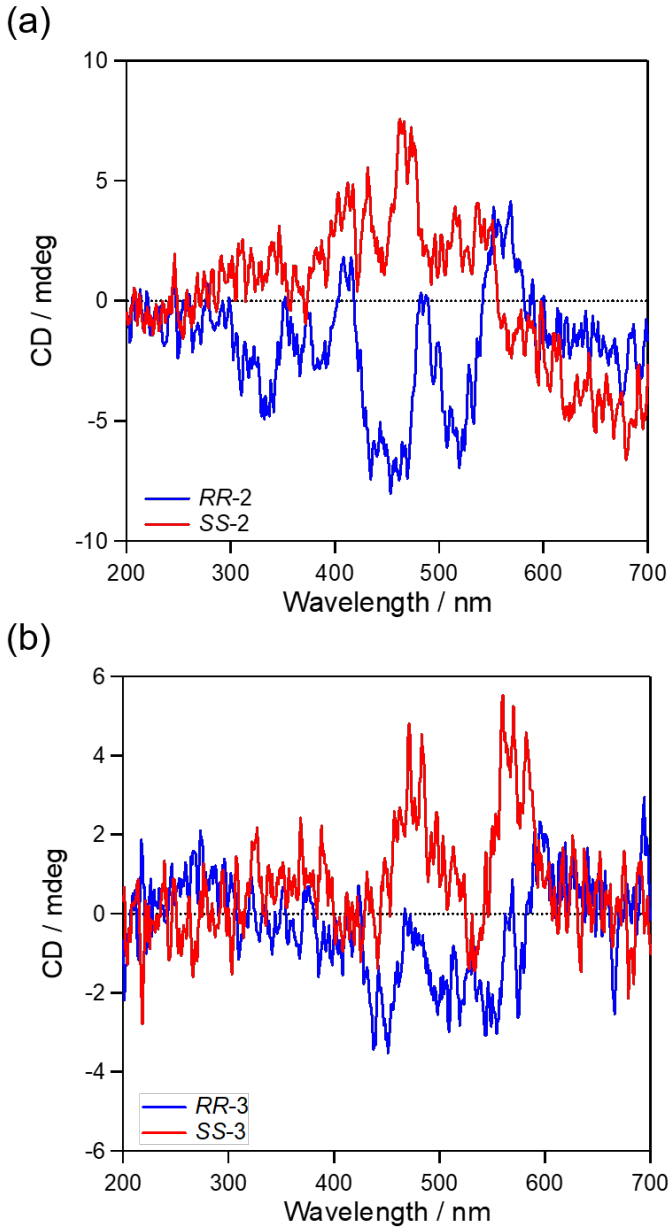

Figure S3. CD spectra of ***SS***/***RR*-2** (a) and ***SS***/***RR*-3** (b) collected in KBr pellet.

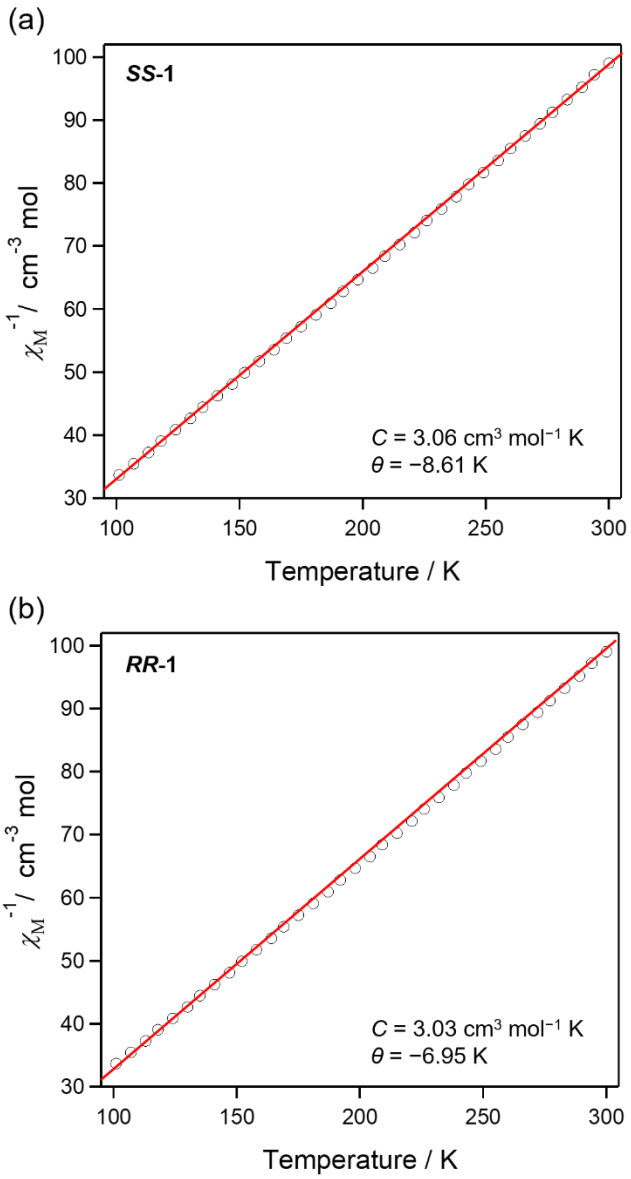

Figure S4. Temperature dependence of χ_M^{-1} for ***SS*-1** (a) and ***RR*-1** (b) in the temperature range 100−300 K under H_{dc} = 1 kOe. The red coloured linear line is the least-squares fitting line based on Curie law.

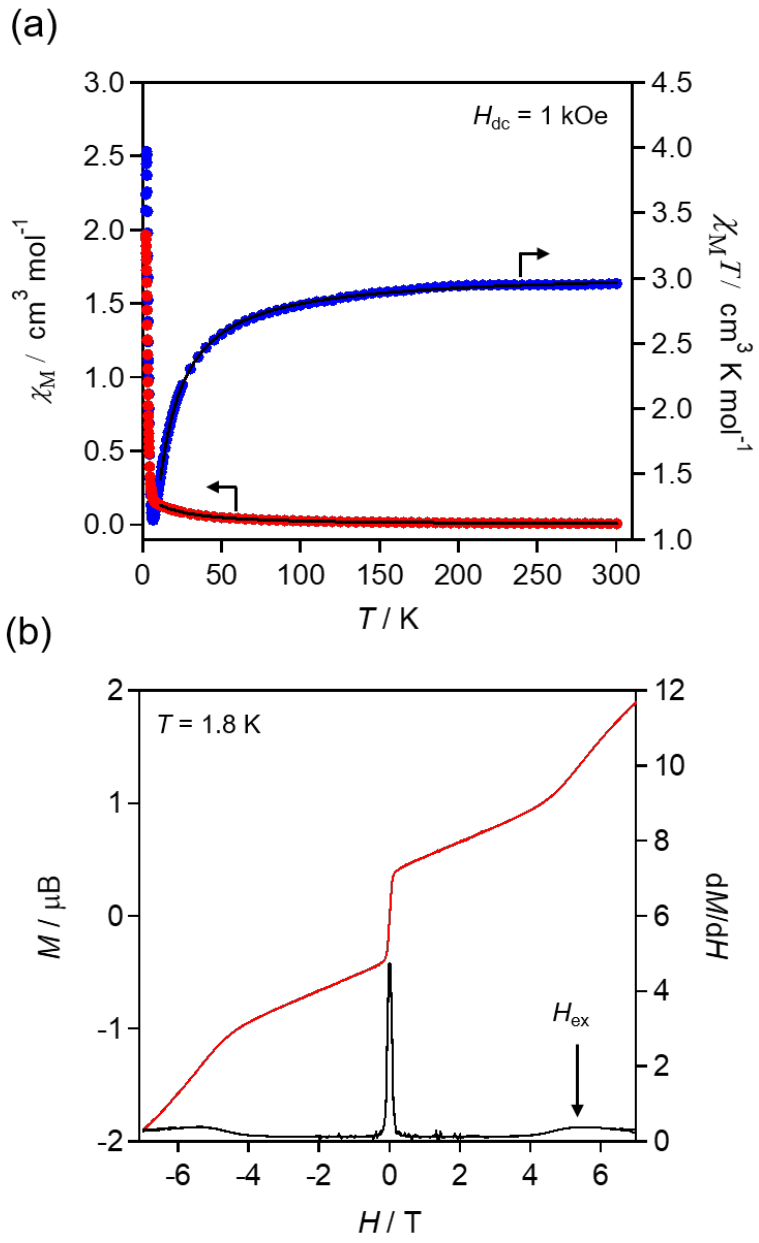

Figure S5. Dc magnetic properties of ***RR*-1**. (a) Temperature dependence of χ_M (filled red circles) and $\chi_M T$ (filled blue circles) under H_{dc} = 1 kOe. The solid black line represents the best fitting line simulated by a Heisenberg $S = 2$ one-dimensional chain model in the temperature range of 9–300 K. (b) Field dependence of magnetization (red line) and the derivative (black line) at 1.8 K.

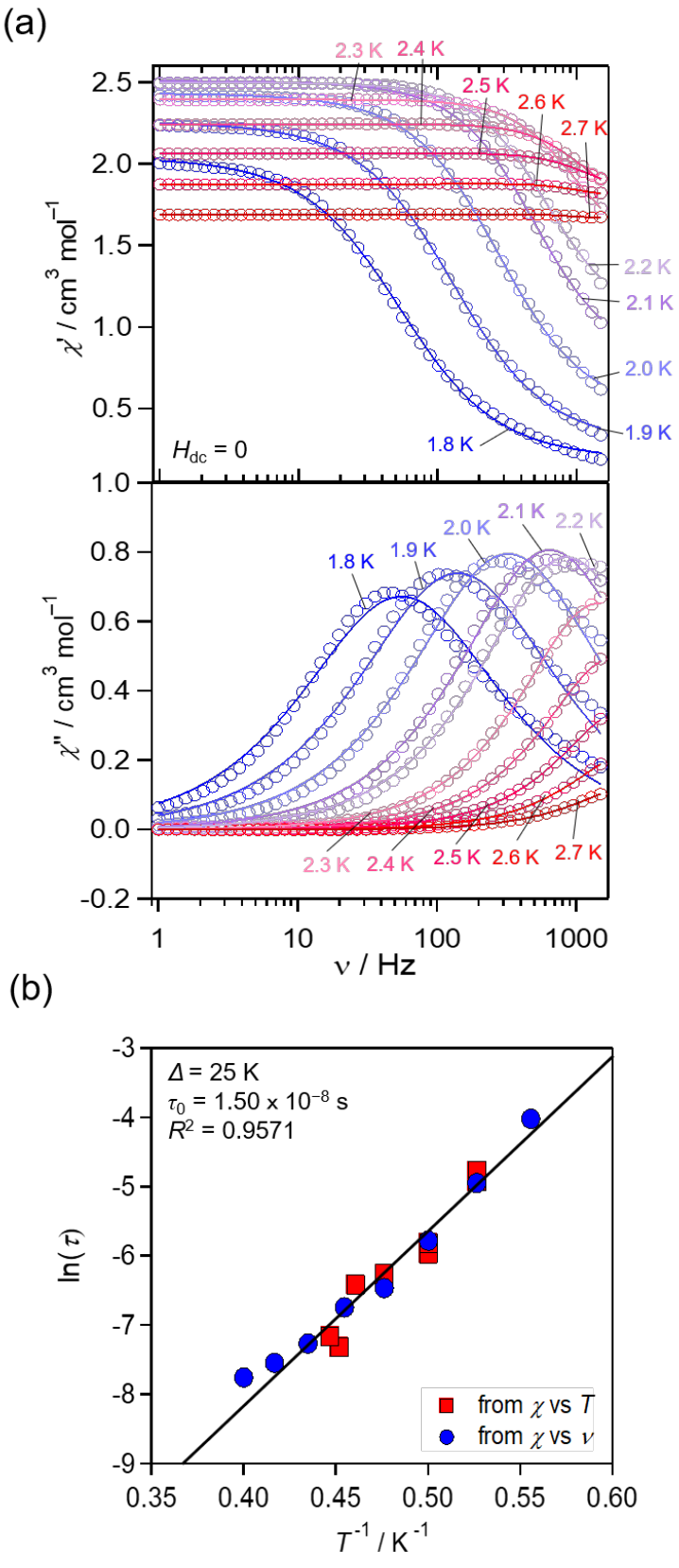

Figure S6. Ac magnetic properties of ***RR*-1**. (a) Frequency dependence of ac magnetic susceptibilities (open circles) with fitting curves (solid lines) and (b) Arrhenius plot of ***RR*-1** with best fit of temperature dependent (red squares) and frequency dependent (blue circles) data shown in black solid line in zero dc magnetic field.

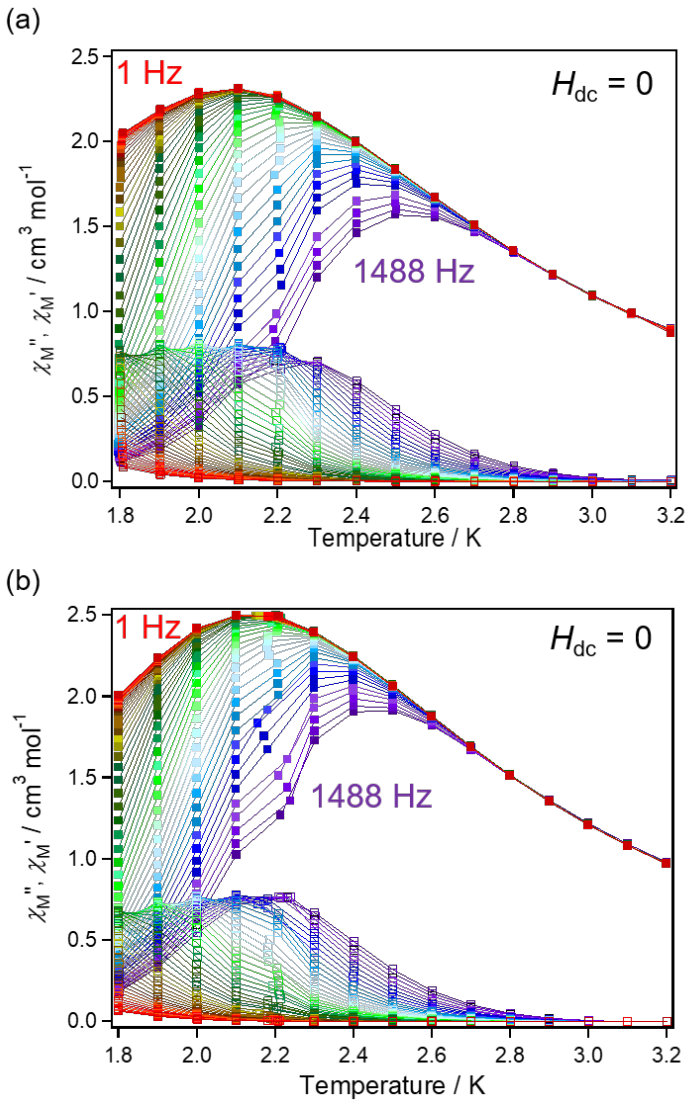

Figure S7. Temperature dependence of real part (filled squares) and imagery part (open squares) ac magnetic susceptibility without external dc magnetic field of ***SS*-1** (a) and ***RR*-1** (b). The frequency of ac magnetic was set between 1 and 1488 Hz.

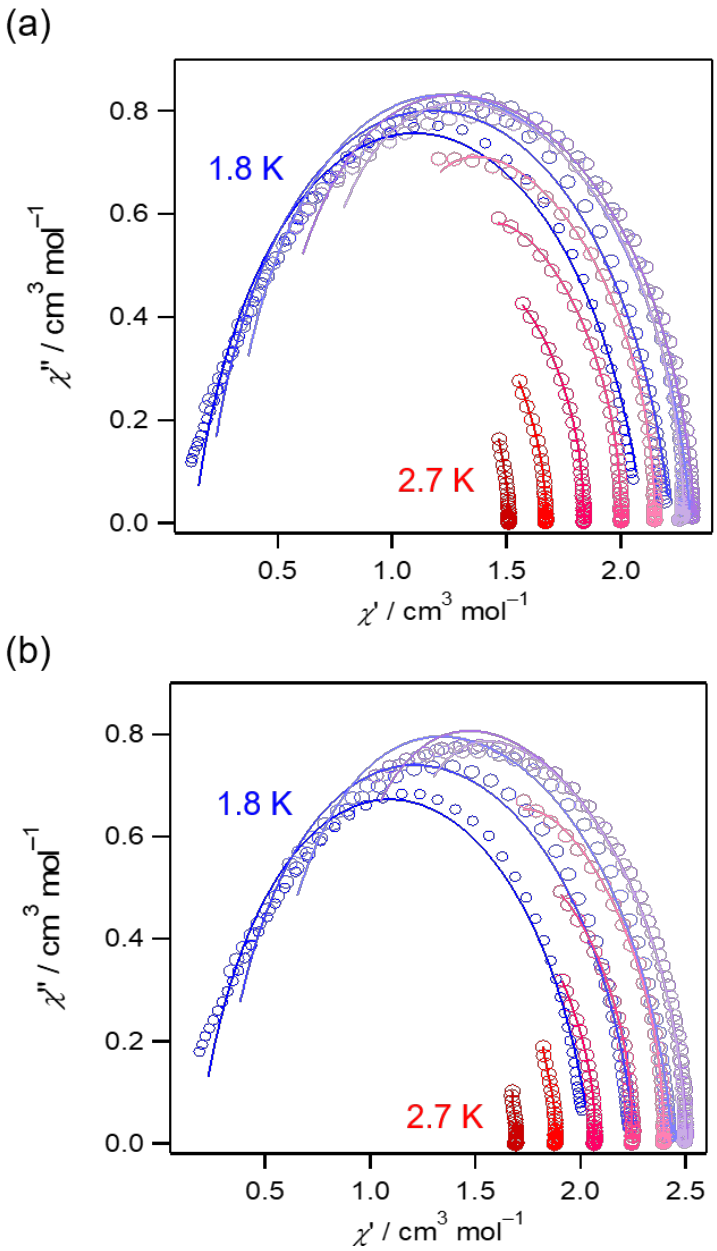

Figure S8. Cole-Cole plot using ac magnetic susceptibilities of ***SS*-1** (a) and ***RR*-1** (b) without external dc magnetic field.

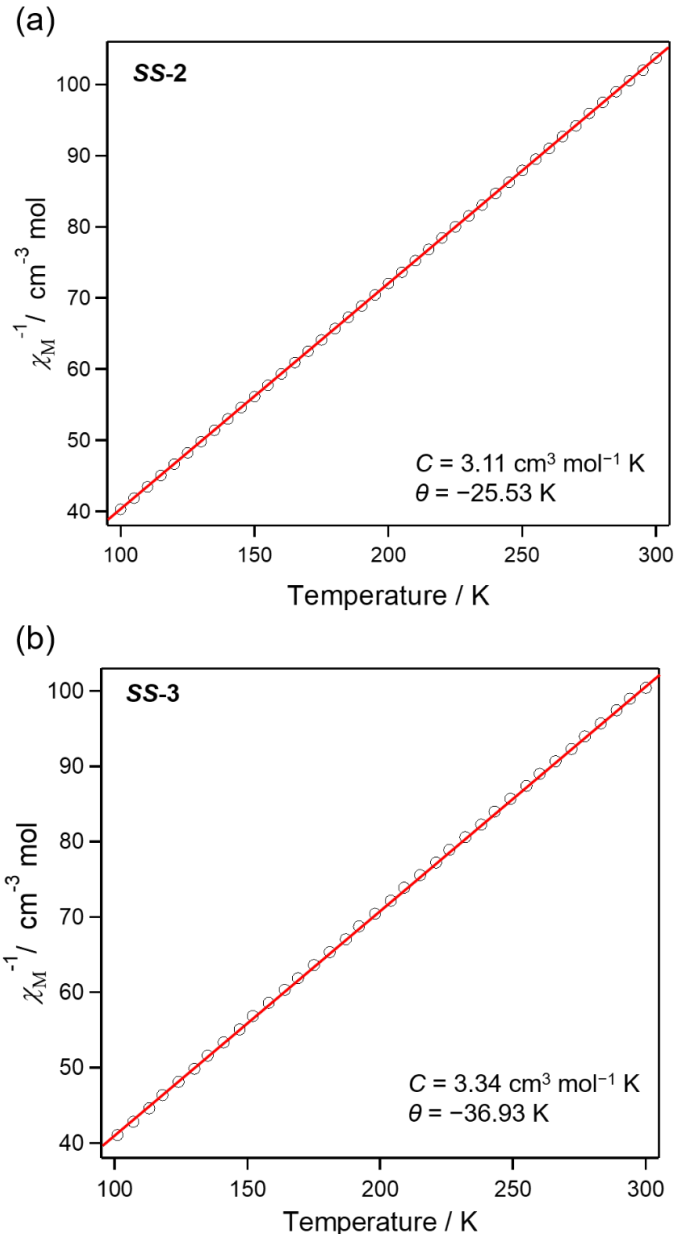

Figure S9. χ_M^{-1} versus temperature of ***SS*-2** (a) and ***SS*-3** (b) at 100−300 K under 1 kOe.

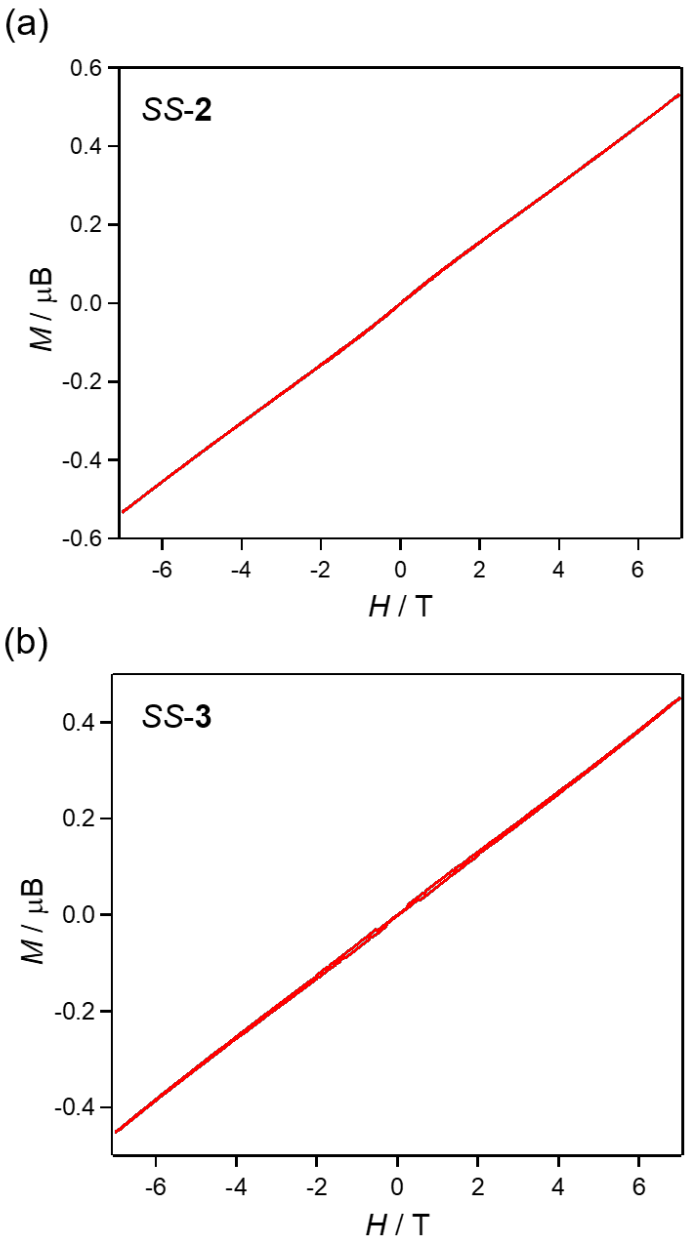

Figure S10. Field dependence of magnetization of ***SS*-2** (a) and ***SS*-3** (b) at 1.8 K.

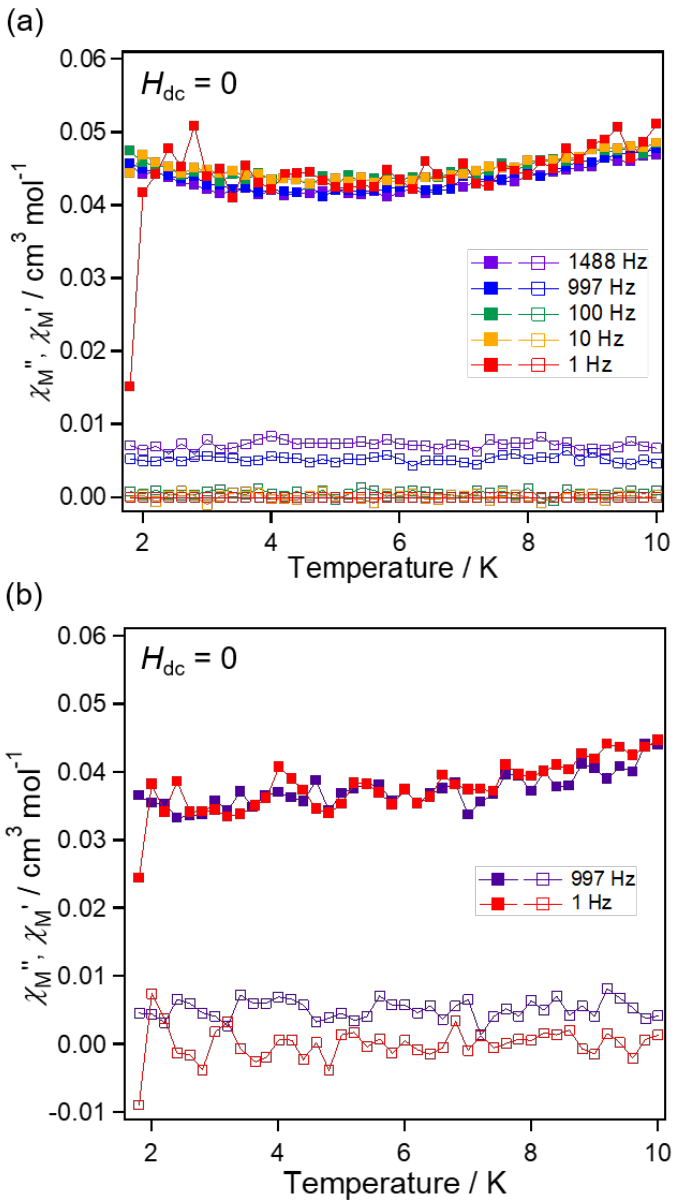

Figure S11. Temperature dependence of real part (filled circles) and imagery part (open circles) ac magnetic susceptibility without external dc magnetic field of ***SS*-2** (a) and ***SS*-3** (b).

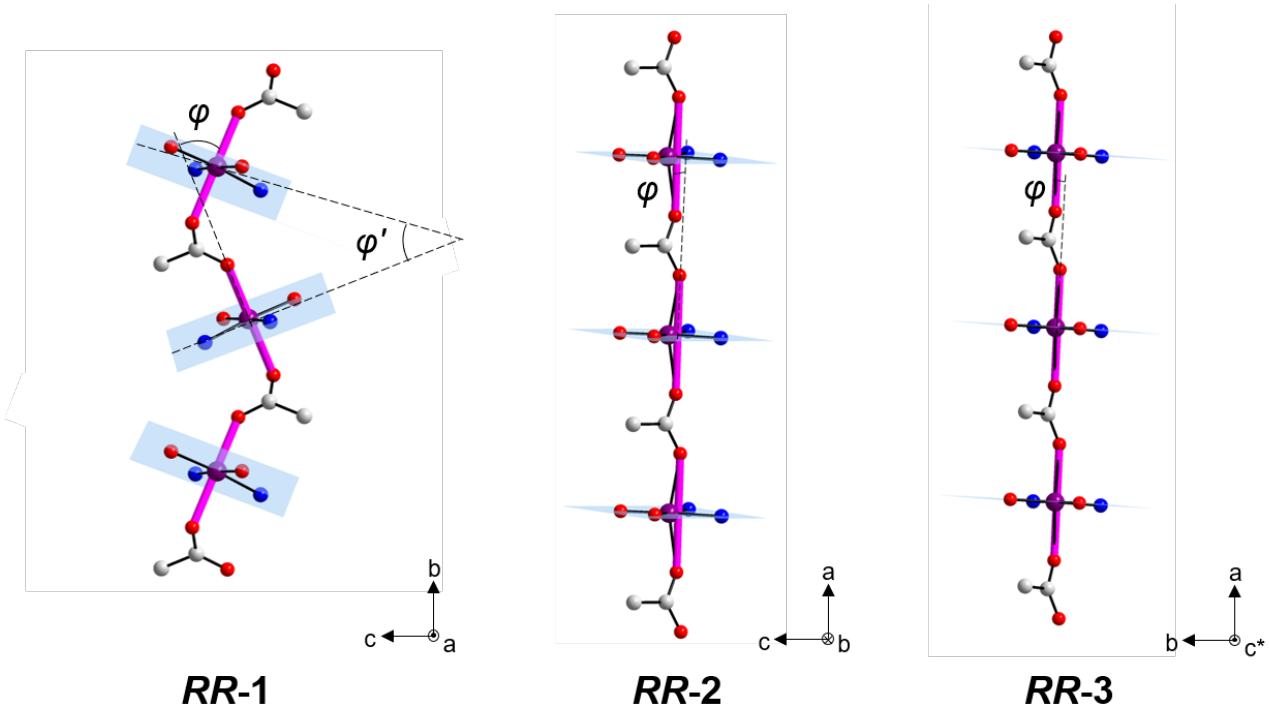

Figure S12. Intrachain canting angle φ between the $O_{ax}\cdots O_{ax}$ axes (pink rods) and plane-to-plane leaning angle φ' between N_2O_2Mn equatorial planes (blue planes) in ***RR*-1**, ***RR*-2**, and ***RR*-3** with C atoms of Xsal-*SS*/*RR*dpeda^{2-} ligand, H atoms, and solvent molecules omitted for clarity.

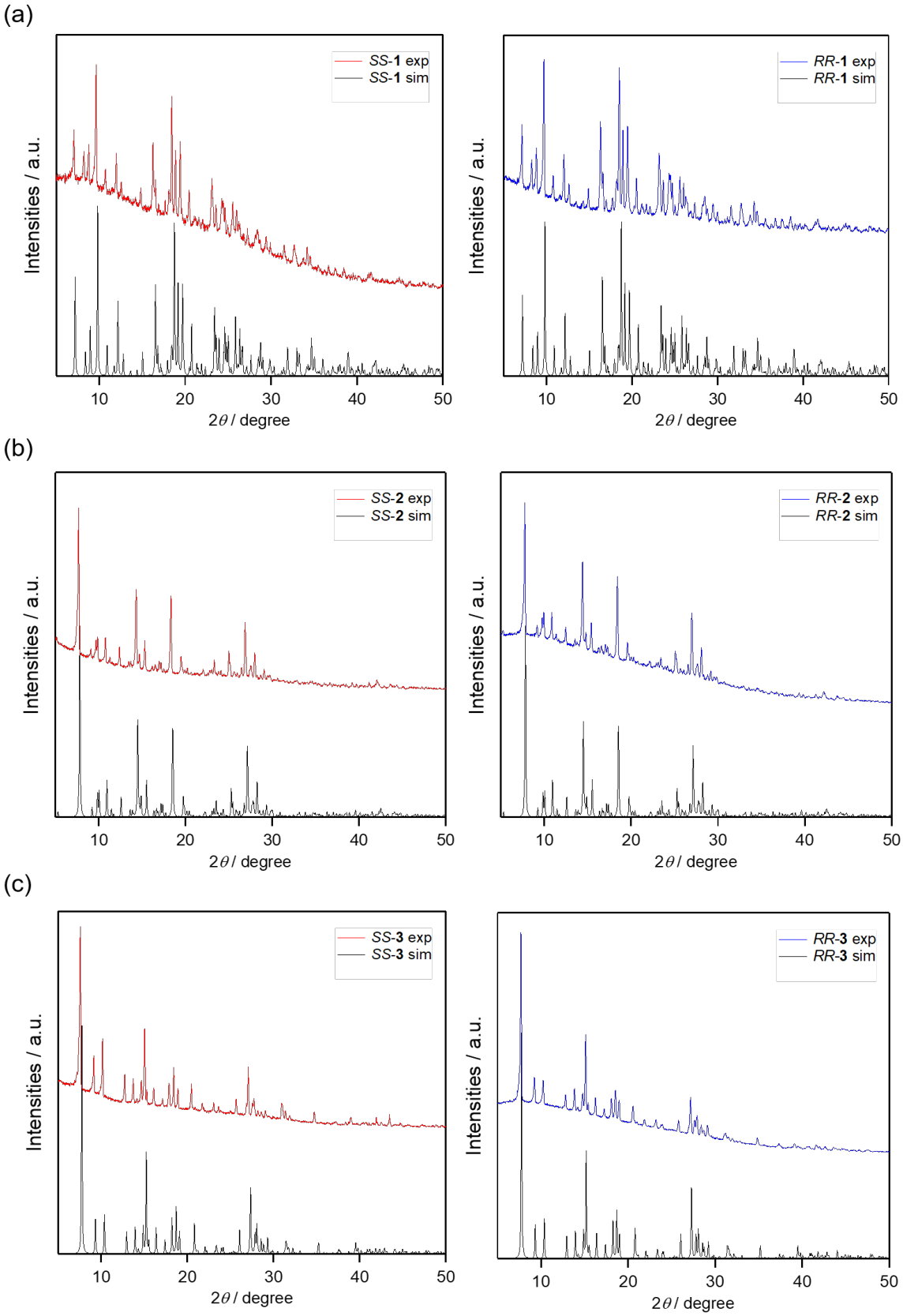

Figure S13. Powder X-ray diffraction patterns of ***SS***/***RR*-1** (a), ***SS***/***RR*-2** (b), and ***SS***/***RR*-3** (c).

Table S1. Crystallographic data for ***SS*-1**, ***SS*-2**, and ***SS*-3**.

	***SS*-1**	***SS*-2**	***SS*-3**
Formula	$C_{31}H_{24.5}Br_2MnN_{2.5}O_4$	$C_{60}H_{46}Cl_4Mn_2N_4O_{8.7}$	$C_{30}H_{23}F_2MnN_2O_{4.5}$
Formula weight	710.79	1213.89	576.44
Crystal system	Tetragonal	Orthorhombic	Monoclinic
Space group	$P4_32_12$	$P2_12_12_1$	$P2_1$
a (Å)	10.7928(3)	6.5703(2)	6.5321(4)
b (Å)	10.7928(3)	17.9817(4)	17.0704(7)
c (Å)	49.2053(11)	45.3393(13)	11.7309(8)
α (°)	90	90	90
β (°)	90	90	103.224(6)
γ (°)	90	90	90
V (Å^3)	5731.7(3)	5356.6(3)	1273.37(13)
Z	8	4	2
T (K)	103	103	103
D_{calc} (g/cm^3)	1.647	1.505	1.503
μ (mm^{-1})	3.290	0.734	0.576
Unique reflns [R(int)]	4699 [0.1698]	10522 [0.1065]	4347 [0.0456]
R_1[a], wR_2[b] [$I>2\sigma(I)$]	0.0749, 0.1182	0.0696, 0.1095	0.0535, 0.0901
R_1, wR_2 (all data)	0.1819, 0.1451	0.1266, 0.1271	0.0889, 0.1008
Flack parameter (x)	−0.030(9)	−0.016(15)	0.002(19)
CCDC No.	2036017	2036018	2036019

[a] $R_1 = (\Sigma||F_O|-|F_C||) / \Sigma|F_O|$, [b] $wR_2 = \{\Sigma [w(F_O^2-F_C^2)^2]/\Sigma [w(F_O^2)]^2\}^{1/2}$

Table S2. Crystallographic data for ***RR*-1**, ***RR*-2**, and ***RR*-3**.

	***RR*-1**	***RR*-2**	***RR*-3**
Formula	$C_{31}H_{24.5}Br_2MnN_{2.5}O_4$	$C_{60}H_{46}Cl_4Mn_2N_4O_{8.7}$	$C_{30}H_{23}F_2MnN_2O_{4.5}$
Formula weight	710.79	1213.89	576.44
Crystal system	Tetragonal	Orthorhombic	Monoclinic
Space group	$P4_12_12$	$P2_12_12_1$	$P2_1$
a (Å)	10.79470(10)	6.57530(10)	6.5420(2)
b (Å)	10.79470(10)	17.9896(4)	17.0906(4)
c (Å)	49.2881(7)	45.3418(7)	11.7543(3)
α (°)	90	90	90
β (°)	90	90	103.659(3)
γ (°)	90	90	90
V (Å^3)	5743.32(13)	5363.35(17)	1277.04(6)
Z	8	4	2
T (K)	103	103	103
D_{calc} (g/cm^3)	1.644	1.503	1.499
μ (mm^{-1})	3.283	0.733	0.574
Unique reflns [R(int)]	7425 [0.0580]	12336 [0.1065]	6322 [0.0236]
R_1[a], wR_2[b] [$I>2\sigma(I)$]	0.0472, 0.0794	0.0391, 0.0794	0.0298, 0.0716
R_1, wR_2 (all data)	0.0670, 0.0845	0.0514, 0.0838	0.0311, 0.0723
Flack parameter (x)	−0.005(4)	−0.013(9)	−0.017(7)
CCDC No.	2036014	2036015	2036016

[a] $R_1 = (\Sigma||F_O|-|F_C||) / \Sigma|F_O|$, [b] $wR_2 = \{\Sigma [w(F_O^2-F_C^2)^2]/\Sigma [w(F_O^2)]^2\}^{1/2}$

Table S3. Selected bond lengths and angles of ***SS*-1** and ***RR*-1**.

	***SS*-1**	***RR*-1**
Mn(1)−O(1)	1.884(5)	1.899(3)
Mn(1)−O(2)	1.904(5)	1.886(3)
Mn(1)−O(3)	2.146(6)	2.147(3)
Mn(1)−O(4)#1	2.196(5)	2.198(3)
Mn(1)−N(1)	2.003(6)	2.004(3)
Mn(1)−N(2)	1.997(6)	1.994(3)
O(1)−Mn(1)−O(2)	94.7(2)	94.79(12)
O(1)−Mn(1)−O(3)	94.1(2)	94.00(12)
O(1)−Mn(1)−O(4)#1	93.5(2)	86.38(11)
O(1)−Mn(1)−N(1)	93.3(2)	91.37(12)
O(1)−Mn(1)−N(2)	173.9(2)	171.68(14)
O(2)−Mn(1)−O(3)	93.8(2)	94.21(12)
O(2)−Mn(1)−O(4)#1	86.6(2)	93.38(12)
O(2)−Mn(1)−N(1)	171.5(3)	173.84(13)
O(2)−Mn(1)−N(2)	91.4(2)	93.05(13)
O(3)−Mn(1)−O(4)#1	172.4(2)	172.34(11)
O(3)−Mn(1)−N(1)	88.3(2)	85.33(12)
O(3)−Mn(1)−N(2)	85.2(2)	88.17(12)
O(4)#1−Mn(1)−N(1)	90.2(2)	87.01(12)
O(4)#1−Mn(1)−N(2)	87.2(2)	90.41(12)
	Symmetry operation	
	#1 1/2–x, 1/2+y, 3/4–z	#1 3/2–x, –1/2+y, 5/4–z

Table S4. Selected bond lengths and angles of ***SS*-2** and ***RR*-2**.

	***SS*-2**	***RR*-2**
Mn(1)−O(1)	1.872(3)	1.874(2)
Mn(1)−O(2)	1.903(3)	1.902(2)
Mn(1)−O(3)	2.205(3)	2.208(2)
Mn(1)−O(4)#2	2.226(4)	2.225(2)
Mn(1)−N(1)	2.000(4)	2.002(3)
Mn(1)−N(2)	1.990(4)	1.996(3)
Mn(2)−O(5)	1.886(4)	1.893(2)
Mn(2)−O(6)	1.891(3)	1.887(2)
Mn(2)−O(7)	2.217(4)	2.213(2)
Mn(2)−O(8)#1	2.233(3)	2.232(2)
Mn(2)−N(3)	1.990(4)	1.995(3)
Mn(2)−N(4)	1.994(4)	1.996(2)
O(1)−Mn(1)−O(2)	93.20(14)	93.24(9)
O(1)−Mn(1)−O(3)	96.45(16)	96.54(10)
O(1)−Mn(1)−O(4)#2	96.89(16)	96.65(10)
O(1)−Mn(1)−N(1)	91.43(15)	91.37(12)
O(1)−Mn(1)−N(2)	174.16(15)	174.06(11)
O(2)−Mn(1)−O(3)	95.13(15)	95.04(10)
O(2)−Mn(1)−O(4)#2	95.78(15)	95.72(10)
O(2)−Mn(1)−N(1)	174.96(16)	174.98(10)
O(2)−Mn(1)−N(2)	92.62(15)	92.68(10)
O(3)−Mn(1)−O(4)#2	162.24(13)	162.44(8)
O(3)−Mn(1)−N(1)	86.31(15)	86.35(10)
O(3)−Mn(1)−N(2)	82.61(16)	82.42(10)
O(4)#2−Mn(1)−N(1)	81.69(15)	81.80(10)
O(4)#2−Mn(1)−N(2)	82.93(16)	83.25(10)
O(5)−Mn(2)−O(6)	92.35(14)	92.74(10)
O(5)−Mn(2)−O(7)	96.64(15)	96.53(10)
O(5)−Mn(2)−O(8)#1	96.97(15)	97.09(10)
O(5)−Mn(2)−N(3)	92.27(16)	91.37(12)
O(5)−Mn(2)−N(4)	174.83(15)	174.85(11)
O(6)−Mn(2)−O(7)	97.18(15)	97.13(10)
O(6)−Mn(2)−O(8)#1	96.56(15)	96.55(10)
O(6)−Mn(2)−N(3)	174.71(17)	174.51(11)
O(6)−Mn(2)−N(4)	92.67(15)	92.24(10)
O(7)−Mn(2)−O(8)#1	160.20(13)	160.17(8)
O(7)−Mn(2)−N(3)	84.83(16)	84.94(10)
O(7)−Mn(2)−N(4)	81.51(16)	81.56(10)
O(8)#1−Mn(2)−N(3)	80.33(15)	80.24(10)
O(8)#1−Mn(2)−N(4)	83.67(15)	93.62(10)
	Symmetry operation	
	#1 –1+x, y, z #2 1+x, y, z	#1 1+x, y, z #2 –1+x, y, z

Table S5. Selected bond lengths and angles of ***SS*-3** and ***RR*-3**.

	***SS*-3**	***RR*-3**
Mn(1)−O(1)	1.878(3)	1.8826(16)
Mn(1)−O(2)	1.878(3)	1.8829(15)
Mn(1)−O(3)	2.200(3)	2.2049(13)
Mn(1)−O(4)#1	2.213(2)	2.2149(13)
Mn(1)−N(1)	1.996(3)	1.9999(18)
Mn(1)−N(2)	1.991(4)	1.9986(18)
O(1)−Mn(1)−O(2)	92.17(13)	92.17(7)
O(1)−Mn(1)−O(3)	97.64(12)	95.30(6)
O(1)−Mn(1)−O(4)#1	97.47(12)	96.34(7)
O(1)−Mn(1)−N(1)	91.75(14)	92.71(7)
O(1)−Mn(1)−N(2)	175.28(14)	175.88(8)
O(2)−Mn(1)−O(3)	95.00(12)	97.79(6)
O(2)−Mn(1)−O(4)#2	96.07(13)	97.29(6)
O(2)−Mn(1)−N(1)	176.02(15)	175.12(8)
O(2)−Mn(1)−N(2)	92.55(13)	91.88(8)
O(3)−Mn(1)−O(4)#2	160.88(10)	160.55(5)
O(3)−Mn(1)−N(1)	85.15(12)	81.77(6)
O(3)−Mn(1)−N(2)	81.88(12)	84.89(7)
O(4)#2−Mn(1)−N(1)	82.74(13)	82.15(6)
O(4)#2−Mn(1)−N(2)	82.09(12)	82.40(7)
	Symmetry operation	
	#1 1+x, y, z	#1 –1+x, y, z

Table S6. Fitting parameter of the dc magnetic susceptibilities of ***SS*-1**, ***SS*-2**, and ***SS*-3**.

	***SS*-1**	***SS*-2**	***SS*-3**
g	2.04(5)	2.04(0)	2.12(0)
J (cm^{-1})	−1.04(2)	−2.67(1)	−3.01(3)
D (cm^{-1})	−1.22(0)	−2.95(7)	−2.24(4)